 doi:10.20944/preprints201712.0087.v1

Pyrolysis Optimization of Agricultural Waste Using Taguchi L9 Orthogonal Array Design

Roberto Antonio Canales Flores [a], Francisco Prieto García [a]*, Elena María Otazo Sánchez [a], Ana María Bolarín Miró [b], Otilio Arturo Acevedo Sandoval [a]

[a] Academic Area of Chemistry, bAcademic Area of Materials and Earth Sciences. Autonomous University of Hidalgo State, Road Pachuca-Tulancingo km 4.5, C.P. 42186. Pachuca, Hidalgo, Mexico.
* Corresponding author. E-mail address: prietog@uaeh.edu.mx (F. Prieto García)

Abstract

This research demonstrates the optimization and production of biochar from barley husk (BH), corn cob (CC), and *Agave salmiana* leaves (AL) via pyrolysis in a muffle furnace. Taguchi experimental design (L9) was applied to conduct the experiments at different levels by altering four operating parameters. Carbonization temperature (300–500 ºC), carbonization time (30–90 min), precursor mass (2–5 g) and N_2 flow rate (100–200 cc/min) were the variables examined in this study. The effect of the parameters on the biochar yield was investigated, and the important parameters were identified employing analysis of variance (ANOVA). The optimum conditions for maximum biochar yield were: carbonization temperature of 400 ºC, carbonization time of 30 min, precursor mass of 2 g, and N_2 flow rate of 150 cc/min. The biochars produced under optimum conditions was characterized physically and chemically. Biochar yields of 19.75% for corn cob (CCB), 32.88% for barley husk (BHB), and 31.14% for agave leaves (ALB) were obtained.

Statement of Novelty

This is the first time reported the obtaining of activated carbon from barley husks and leaves of *agave salmiana*

Keywords: pyrolysis; biomass; biochar; Taguchi; optimization

 doi:10.20944/preprints201712.0087.v1

1. Introduction

Lignocellulosic biomass is a complex biological product and is considered as a promising alternative and a renewable energy source that can be transformed by thermal processes into other value-added products such as biochar and bio-oil. (Stefanidis et al., 2014; Tripathi et al., 2016).Significant researchers have been devoted to the production of carbonaceous materials from agricultural waste (Ioannidou and Zabaniotou, 2007). Wood, corn straw, olive stones, bagasse, sugar cane bagasse, almond shells, corn stover, apricot stones, nut shells, corn cob, rice husk and rice straw are some examples of biomass used for obtaining biochar (Canales-Flores and Prieto-García, 2016).

Conversion of biomass into biochar can be made mainly by two methods: pyrolysis and gasification (Ahmad et al., 2014). Of the two methods mentioned, pyrolysis is the most used method to produce biochar from the biomass (Canales-Flores and Prieto-García, 2016; Tripathi et al., 2016). On the gasification method, the biomass is heated to temperatures above 700 °C to obtain gases rich in carbon monoxide and hydrogen, under controlled oxygen or vapor conditions (Ahmad et al., 2014). In contrast, on the pyrolysis, the lignocellulosic material is thermally degraded at temperatures in the range of 200-900 °C under an inert atmosphere to produce biochar, bio-oil, and gas (Ahmad et al., 2014; Tripathi et al., 2016). Biochar is one of the by-products obtained from the thermal degradation of lignocellulosic matter(Tripathi et al., 2016), and it is descriptivelydefinedbyShackley et al. (2012)as ‘‘*the porous carbonaceous solid produced by the thermochemical conversion of organic materials in an oxygen depleted atmosphere that has physicochemical properties suitable for safe and long-term storage of carbon in the environment*.”

According to Tripathi et al. (2016), the production of biochar from biomass does not only depend upon the technique employed to produce, but it is also a function of the process parameters. Research on the pyrolysis has revealed that the production, yield, and properties of the biochar depend upon several factors like biomass properties (moisture content and particle size), reaction conditions (temperature, time, and heating rate) and another factors (flow rate of carrier gas, catalyst, and reactor type) (Tripahi et al., 2016). These authors also indicate that itto achieve maximum yield of biochar, the process parameters of the biomass pyrolysis have to be optimized.

 doi:10.20944/preprints201712.0087.v1

Biochar production from biomass requires consideration of various factors. The use of statistical designs of experiments has been implemented in several optimization studies to determine which factors affect the process and to reduce the number of trials significantly (Loloide et al., 2016; Syed-Hassan and Md Zaini, 2016). Taguchi methodology is widely used in the design and optimization of experiments and uses orthogonal arrays to organize control factors and the levels at which each factor is evaluated (Syed-Hassan and Md Zaini, 2016). Taguchi design evaluates pairs of combinations to determine the optimum levels that contribute to optimum response value taking into account the mean value, the variance and the signal-to-noise (S/N) ratio (Syed-Hassan and Md Zaini, 2016).

In this study, Taguchi orthogonal array design was implemented as a systematicmethod to obtainoptimum conditions for the preparation of biochar by pyrolysis of barley husk, corn cob, and agave leaves. This design was employed with the objective ofmaximizing the biochar yields. The effect of the process parameters such as carbonization temperature process time, precursor mass, and N_2 flow rate, was examined. Comparisons of biochar's physical and chemical characteristics were also made.

2. Materials and methods

2.1. Preparation of precursors

Barley husk (BH), corn cobs (CC), and *Agave salmiana* leaves (AL) were the lignocellulosic residues used a biochar precursors in this study. These precursors were obtained from Almoloya and Apan in the State of Hidalgo, Mexico. The raw materials were washed five times with distilled water, titrated in a food processor, dried at 105 ºC for 72 h in an oven, ground in a knife mill to obtain 0.3-1.0 mm particle size and finally sieved through 18 and 45 mesh sieves.The chemical composition of BH, CC, and AL is summarized in Table 1. Chemical characterization of the precursors was carried out according to the method described in ASTM Standard D3172 (1997), total sugars and fat according to the TAPPI T204 (1997), Klason lignin according to the TAPPI T222 (1998), holocellulose according to the method described by Wise et al. (1946), and α-, β- and γ-cellulose according to the TAPPI T203 (1999).

Preprints (www.preprints.org) | NOT PEER-REVIEWED | Posted: 14 December 2017 doi:10.20944/preprints201712.0087.v1

Table 1. Chemical composition of precursor (%wt.)

Precursor	Lignin	α-cellulose	β-cellulose	γ-cellulose	Holocellulose	Sugars	Fat
BH	26.46	66.69	22.38	10.92	82.07	27.44	2.06
CC	15.24	52.60	44.52	2.89	82.38	19.34	0.82
AL	15.58	79.45	13.18	7.37	83.05	42.29	1.68

2.2. Preparation and characterization of biochar

Carbonization of the three precursors was performed in a muffle furnace with nitrogen gas with a 99.999% purity to completely purge the air from the reaction environment for 30 minutes, and a allow the pyrolysis process to proceed in the absence of oxygen. The muffle furnace was then turned on, and the temperature was elevated at a constant heating rate of 20 ºC/min until the final carbonization temperature was reached. The system was maintained at the carbonization temperature for a particular period called carbonization time. Finally, the system was cooled to room temperature under nitrogen flow, and the biochar obtained was removed from the furnace. The yield of biochar production was calculated as follows:

$$\text{Yield } (\%) = \frac{W_2}{W_1} \text{ x } 100$$

where W_1 is the initial weight of the precursor (g), and W_2 is the weight of the obtained biochar (g).

2.3. Taguchi experimental design

Experimental design is a powerful approach for the optimizationof parameters. Taguchi methodis one of the most tried-and-true, fastest techniques for design ofexperiments and response optimization. The Taguchi design is based on testing the sensitivity of a set of response variables to a set of control parameters by considering experiments in an orthogonal array with an aim to attain the optimum setting of the control parameters or factors. In this research L9 orthogonal array with four operational parameters known as control factors, namely carbonization temperature (ºC), carbonization time (min), precursor mass (g) and N_2 flow rate (cc/min), with three levels for each as shown in Table 2. In the

Preprints (www.preprints.org) | NOT PEER-REVIEWED | Posted: 14 December 2017 doi:10.20944/preprints201712.0087.v1

Taguchi method, there are three main types of S/N ratio, which are smaller the better, nominal the best, and larger the better. Since the aim of this study is to obtain the value of response (biochar yield) as high as possible, the larger the better is used. Noise factor taken in this study is the raw material. BH is considered as the noise factor 1, CC is taken as noise factor 2, and AL is considered as noise factor 3. Table 3 shows the L9 orthogonal array including the noise factors. The design matrix was provided by ANTM 2.5, a statistical software which incorporates Taguchi's L9 Orthogonal Array Method. This software was also used in the computation of the ANOVA.

Table 2. Control factors and their levels.

Process parameters	Level 1	Level 2	Level 3
Factor A: Carbonization temperature (ºC)	300	400	500
Factor B: Carbonization time (min)	30	60	90
Factor C: Precursor mass (g)	2	3	5
Factor D: N_2 flow rate (cc/min)	100	150	200

Table 3. Orthogonal array (L9) of Taguchi experimental design with the noise factors and the measured yield value of biochar.

Inner control factor control array					Outer noise factor array		
Run	Process parameters				Yield (%wt.)		
	Factor A (ºC)	Factor B (min)	Factor C (g)	Factor D (cc/min)	BHB	CCB	ALC
1	300	30	2	100	34.49	18.36	39.3
2	400	60	3	200	19.10	5.16	15.43
3	500	90	5	150	16.21	3.20	33.04
4	300	60	3	200	33.87	9.87	34.15
5	400	90	2	150	19.71	3.46	18.73
6	500	30	5	100	26.02	13.7	21.99
7	300	90	5	200	25.61	9.15	26.47
8	400	30	2	150	26.67	4.76	29.48
9	500	60	3	100	17.04	3.94	17.71

 doi:10.20944/preprints201712.0087.v1

2.4. Characterization of biochar

The optimum biochars were characterized according to the method described in ASTM Standard D3172 (1997). Elemental analyses of C, H, and N was carried out by a Perkin Elmer analyzer model 2400 PECHN-SO using acetanilide as the reference. The oxygen content was obtained indirectly by difference. The thermal behavior was performed with a Mettler-Toledo analyzer model TGA/SDTGA-851, under a nitrogen atmosphere, with a heat ramp of 10 ºC/min up to 600 ºC. Besides, the biochars were analyzed by Fourier Transform infrared spectrophotometry (FTIR) on a Perkin Elmer Spectrum one spectrometer. The spectra were recorded in the region of 4000 to 370 cm^{-1}, resolution of 4 cm^{-1} and ten scans. The surface morphology of the precursors was observed by scanning electron microscopy (SEM) using a JEOL scanning electron microscope model JSM 6300 operated at 10 kV. For observation, particles of the precursors were dispersed onto carbon tape and coated with gold. X-ray powder diffraction (XRD) in a Bruker D2 Phaser 2nd Gen, for values of 2θ from 5° to 70° using Cu *K*α radiation (1.54184 Å), and a detector Lynxeye (ID mode).The pore distribution was determined by mercury porosimetry in a porosimeter Model AutoPore IV 9500 with detection range of 0.003 µm to 360 µm, and potential Z on a Malvern Zetasizer nanoseries.

3. Results and discussion

3.1. Analysis of variance (ANOVA) of S/N ratio and effects of the control factors on the biochar preparation

According to Taguchi orthogonal array, twenty-seven different biochars were prepared. Table 3shows the yield results of biochar for each run, and are used to predict the optimum condition for the process pyrolysis. Yield results between 16 to 34% for BHB, from 3 to 18% for CCB, and from 15 to 39% for ALB were obtained. The S/N ratio was tested by ANOVA to determine the relative significance of the S/N data obtained for the process parameters. According to Kundu et al. (2014), ANOVA determines the impact of the independent variableson the dependent variables in a regression analysis. The ANOVA results for S/N ratio are given in Table 4. Effects of control factors on the S/N ratio of the biochar yields can be observed in Figure 1.Bold values in Table 4 for the level averages are

 doi:10.20944/preprints201712.0087.v1

the maximum average S/Nperformances of factors in the four different levels at each factor.F-value indicates the statistical calculation on the effects of control factor to the response. The F-value is obtained by comparing the variance associated with the residual variance. The factor with high F-value is themost important factor affecting the yield of biochar. According to Kirby (2006), a F-ratio lessthan one suggests insignificant effect, a value near about two suggestsmoderate effect and if the F-ratio is more than four, thecontrol factors have a strong and significant effect on the response. Therefore, Table 4 shows that the carbonization time and the precursor mass have a significant effect on the preparation of biochar whereas the N_2 flow rate and the carbonization temperature have a moderate effect. The S/N ratio for the carbonization time increases as the level decreases from 90 min to 30 min, meaning that the biochar yield increased. However, when the carbonization time was higher than 30 min, the S/N ratio decreased, indicating that the biochar yield decrease. Prías-Baragán et al. (2011) found that low temperatures with extended carbonization times are required to improve activated carbon production.It means that by increasing the carbonization times, it is promoted to the repolymerization of the constituents of the biomass by giving them sufficient time to react.On the other hand, if the carbonization times are very short, the repolymerization of the components of the biomass will not be completed, and the biochar yields will be decreased. The S/N ratio indicated that the optimum level for the carbonization time is the level 1 which corresponds to 30 min.Practically no change wasobserved in the S/N ratio for the last two levels of carbonization time of 60 min and 90 min.During the experimentation, it was observed that increasing the carbonization time with high temperatures resulted in a decrease in biochar yield.Thus, the shorter carbonization time in combination with moderate temperatures had a very significant effect for obtaining higher biochar yields. The increase in the biochar yield at the first level of carbonization time was due to the release of the volatile components from the precursors is gradual, and the repolymerization reactions take place(Tripathi et al., 2016).

Preprints (www.preprints.org) | NOT PEER-REVIEWED | Posted: 14 December 2017 doi:10.20944/preprints201712.0087.v1

202 **Table 4.** ANOVA S/N ratios for the prepared biochars.

Source	DF[a]	S[b]	V[c]	F	S´[d]	P[e] (%)	Level average		
							Level 1	Level 2	Level 3
Factor A (ºC)	2	8.60	4.30				20.41	**21.52**	19.12
Factor B (min)	2	105.01	52.50	12.21	96.40	50.23	**25.10**	17.22	18.74
Factor C (g)	2	61.26	30.63	7.12	52.65	27.43	**23.88**	19.51	17.66
Factor D (cc/min)	2	17.07	8.53	1.98	8.46	4.41	19.94	**22.21**	18.91
Residual error	2	8.60	4.30		34.40	17.93			

203 [a] DF: degree of freedom.
204 [b] S: standard deviation.
205 [c] V: variance (S^2).
206 [d] S´: standard deviation recalculated by neglecting the smallest variance.
207 [e] P: contribution percentage at each factor.
208
209

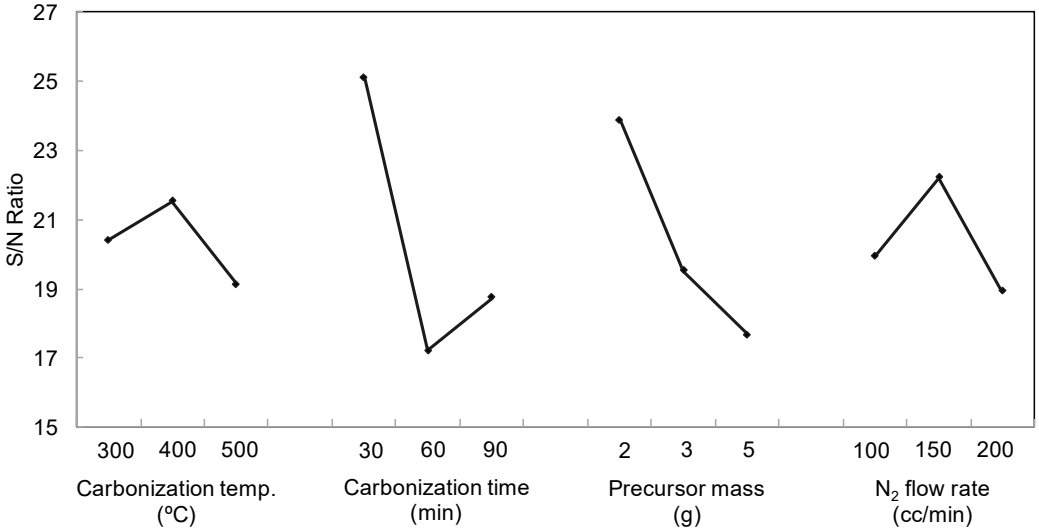

210
211 **Figure 1.** Effect of the control factors on the S/N ratio of the biochar yield.
212

213 The literature also mentions that the effect of the carbonization time is directly related to
214 other process parameters such as the carbonization temperature and the heating rate. Table
215 4 shows the S/N ratio for the carbonization temperature which increases the biochar yield in
216 the level 2 which corresponds to 400 ºC. This carbonization temperature was the best for
217 obtaining the highest carbon yieldsbecause high temperatures promotethe thermal cracking
218 of heavy hydrocarbons present in the precursorincreasing the liquid and gaseous products,
219 and the decrease of biochar yield (Tripathi et al., 2016). These findings are consistent with
220 those reported byAteş et al. (2004) who showed that a temperature increase of 400 to 700

 doi:10.20944/preprints201712.0087.v1

°C caused a 17% reduction in the yield of biochar for sesame stems. Choi et al. (2012) also reported the decrease of the biochar yield with increasing pyrolysis temperature.

Table 1 shows that the three precursors presented high contents of α-cellulose and low contents of lignin, with values of 52.60-79.45% and 15.58-26.46%, respectively.The literature indicates that, during pyrolysis processes, low temperatures are suitable for cellulose-rich precursors, because at high temperatures (>800 °C) cellulose leads to the formation of volatile products while at low temperatures (450-600 °C). It is lead to the formation of biocharsince the cellulose is degraded to anhydrocellulose resulting in the high production of biochar.Therefore, carbonization temperature of 400 ºC was adequate to obtain higher biochar yields.

The rate of entrainment gas flow is another important parameter in the pyrolysis process.The S/N ratio indicated that 150 cc/min is the optimum level for the N_2 flow rateduring the pyrolysis process. This result is consistent with studies by Sensöz and Angin (2008), who found that biochar yield decreased with increased the rate of nitrogen flow during the pyrolysis process of safflower seeds. They concluded that once the flow of nitrogen exceeds 100 cc/min, the yield of biochar remains almost constant. Zhang et al. (2009) found that there is no noticeable change in biochar yield by increasing the nitrogen flow rate above 2.3 L/min. The studies by Onay et al. (2001) and Pütün et al. (2002) found that there is no significant change in biochar yield by increasing the nitrogen flow rate above 50 cc/min. These findings indicate that a low nitrogen flow rate is sufficient to take most of the vapors out of the reaction zone resulting in high biochar yields. Therefore, a N_2 flow of 150 cc/min is suitable for the process since, according to the authors, high flow rates of nitrogen are not necessary to obtain high biochar yields.

Concerning the effect of the mass of the precursor, it was found that 2 g is the optimal condition for obtaining the higher yield of biochar since with this amount of precursor the release of the volatile components is optimal in combination with short carbonization times (30 minutes).

3.2. Optimization of the process parameters

In this study, the “larger the better” type ofanalysis was selected as the response since the highest biochar yield is alwaysdesirable. The largest S/N ratio corresponds to the optimum

 doi:10.20944/preprints201712.0087.v1

252 characteristics. Table 4 shows the mean S/N ratio for each level of the control factors,
253 which wassummarized as S/N response. As can be seen in Figure 1, the optimum condition
254 is the following:carbonization temperature of 400 ºC (level 2), process time of 30 min
255 (level 1), precursor mass of 2 g (level 1), and N_2 flow rate of 150 cc/min (level 2). For the
256 additional study, biochar samples were prepared by confirmatory experiments using these
257 levels for the control factors. Biochar yields of 19.75% for CCB, 32.88% for BHB, and
258 31.14% for ALB were obtained under optimum conditions. These biochars were
259 characterized physically and chemically.
260
261 **3.3. Characterization of the biochars obtained under optimum conditions**
262 According to Nieto-Delgado et al. (2011) to consider a raw material as a good precursor to
263 produce activated carbon must possess certain characteristics such as low cost, availability,
264 high carbon content, low content of inorganic compounds, and the existence of a natural
265 porosity. Figure 2 shows the results of proximal analysis of biocharscompared with the
266 precursors. As illustrated, the moisture content of the precursors was the same, around 7%,
267 and for the biochars was less than 4%. Tripathi et al. (2016) mention that low moisture is
268 advisable for the activated carbon production because it not only reduces the heat energy
269 but it also lowers the time required for the process. Specifically, lignocellulosic precursors
270 with more than 30% of moisture are not suitable for the pyrolysis since the greater amount
271 of energy supplied to the biomass would be used in moisture removal present in it and rest
272 would be used to increase its temperature. They also indicate that a significant amount of
273 moisture (more than 40%) reduces the heating rate resulting in more time in achieving the
274 process temperature. Demirbas (2004) and Xiong et al. (2013) observed that increase in
275 moisture content in pyrolysis of wood and sewage sludge, respectively, decreases the yield
276 of biochar. Therefore, the moisture content of the three precursors of this study was suitable
277 for the biochar production under optimum conditions.
278 Ash content is another important parameter in the activated carbon production since it
279 defines the quality of precursor in the combustion determining the content of incombustible
280 matter and it is related to the dissolution of salts generating problems of pollutantsin
281 aqueous mediawhen the activated carbon is used. (Nieto-Delgado et al., 2011). Thus, a low
282 ash content is desired because it could negatively affect the yields to partially eliminate the

Preprints (www.preprints.org) | NOT PEER-REVIEWED | Posted: 14 December 2017 doi:10.20944/preprints201712.0087.v1

283 formation of char (Pereira et al., 2014).In this research, the ash contents of precursors are
284 less than 10% and are acceptable for the activated carbons production. In contrast, the ash
285 content of CCB and ALB was the same, around 33%. However, the ash content of BHB
286 was higher, about 45%. In this case, we established that the yield of the BHB is masked by
287 the high content of inorganic compounds.It is attributed to the fact that barley by holding
288 the grass family has a natural tendency to absorb a significant amount of silicon (Espino et
289 al., 2014), which is concentrated after the heat treatment.
290

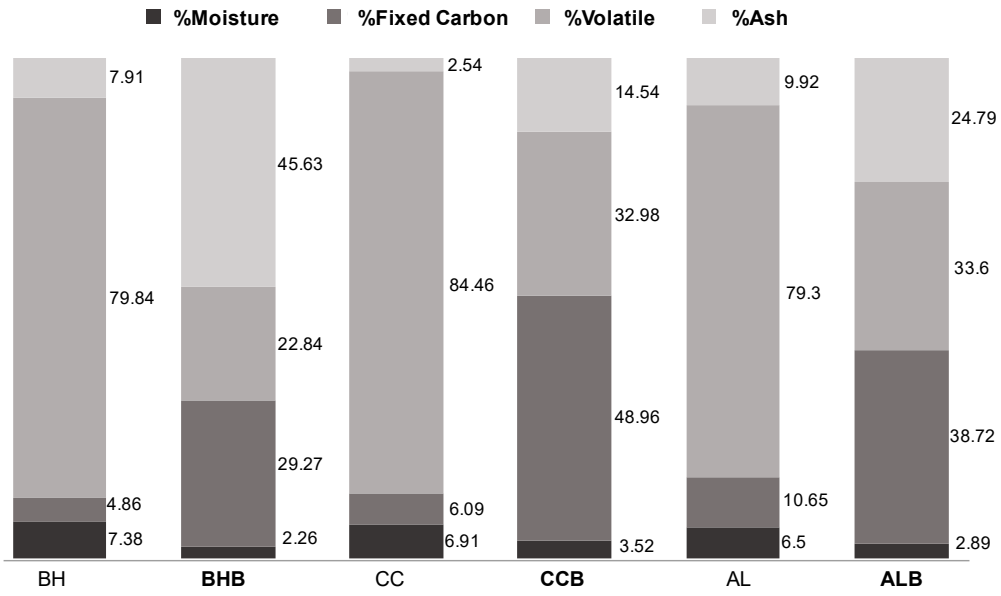

291

292 **Figure 2.** Proximal analysis of biochars obtained under optimum conditions and precursors.
293

294 Regarding the content of volatile matter, the volatile matter content is another important
295 parameter because it indicates the reactivity and ease of ignition of an organic material
296 (Canales-Flores and Prieto-García, 2016).In this study, high volatile contents were found on
297 the precursors with values from 79% to 84%.These values are very suitable for the process
298 pyrolysis since the gradual and controlled release of volatile matter, result in the enrichment
299 of carbon (Canales-Flores and Prieto-García, 2016). In contrast, contents of volatile matter
300 from 22% to 33% were determined for the biochars. These results are lower than those of
301 the raw materials.This tendency was to be expected since the gradual and controlled loss of
302 volatile matter under optimum conditions, produced the carbon enrichment in the biochar

Preprints (www.preprints.org) | NOT PEER-REVIEWED | Posted: 14 December 2017 doi:10.20944/preprints201712.0087.v1

obtained, mainly in CCB (48.96%) and ALB (38.72) as shown in Figure 3. The BHB showed the lowest carbon enrichment due to its high content of inorganic material.

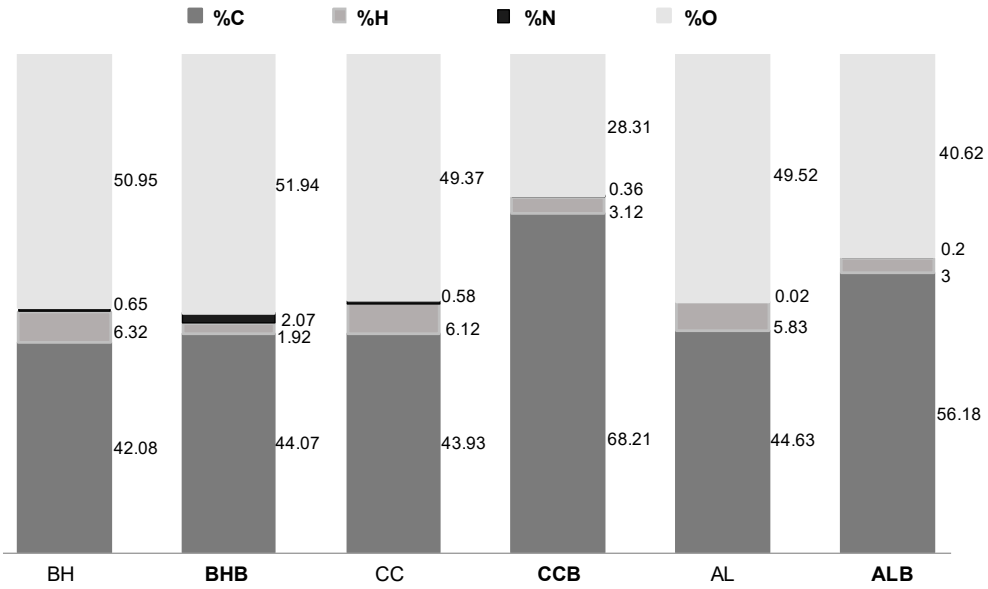

Figure 3. Elemental analysis of biochars obtained under optimum conditions and precursors.

3.4. Fourier-transform infrared spectroscopy (FTIR)

FT-IR spectra of the BH compared with BHB, CC compared with CCB, and AL compared with ALB are shown in Figure 4A-C. The intenseband is appearing at 3400 cm^{-1} in all samples, was attributed to stretching vibrations, characteristic of the hydroxyl functional group (O–H)belonging to the cellulose structure, which is themajor component of the precursors. The band characteristic of the methyl group resultant of (C–H) asymmetric and symmetric stretching was assigned to olefiniccompounds, which suggests an aliphaticity in the structure of the precursors. It was observed that the three precursors present diverse functionalgroups such as esters, ethers, alcohols, aldehydes, ketones, phenolsand carboxylic acids. Thus, in the double bond region, a shoulder peak at 1733 cm^{-1} for BH, at 1737 cm^{-1} for CC, and at 1731 cm^{-1} for AL, were assigned to the C=O stretching of the acetyl and uronic ester groups of hemicellulose, and to the ester linkage of carboxylic group of the *p*-coumaric acid of lignin.

 doi:10.20944/preprints201712.0087.v1

These bands disappeared in the spectra of the three biochars (Figure 4A-C). In contrast, It can be observed that there are few differences about the peak assigned to the primary amines in both precursor and biochars. Bledzki et al. (2010) mention that the exact frequency of this vibration depends on the nature of the hydrogen bonds in the C=O and N-H groups. Thus, a peak at 1626 cm^{-1} (more intense) for BHB (Figure 4A), at 1595 cm^{-1} (low intensity) for CCB (Figure 4B) and at 1612 cm^{-1} (shoulder) for ALB (Figure 4C) were observed.

Bands in the range of 1375-1350 cm^{-1} were assigned to the symmetrical and asymmetric deformations of C-H in methyl and phenolic alcohol. The bands at 1458 cm^{-1} for BHB, from 1379 to 1053 cm^{-1} for CCB, and from 1418 to 1059 cm^{-1} for ALB, were assigned to deformation vibrations of C-C in aromatic rings, as well as to the vibrations of C-O and C-H. According to Bohli et al. (2015), this region is indicative of the carbon enrichment after heat treatment.

A sharp peak at around 900 cm^{-1}, characteristic of β-glycosidic linkages between the sugar units of the cellulose (Bledzki et al., 2010), disappeared in the three biochars as a result of pyrolysis. As can be seen, this region of bands, characteristic of the components of the cellulose, presented substantial changes after obtaining the carbonaceous materials under optimum conditions.

Analyzing the spectrum of the BHB sample, it can be observed that there are three major differences about the spectrum of the CCB and ALB, associated with intense peaks at 1091 cm^{-1}, 796 cm^{-1}, and 450 cm^{-1}.The first two bands are indicative of the vibrations of the Si-O-Si bond bonds, and the third is assigned to the flexion of the O-Si-O bonds (Shen et al., 2014). This finding is consistent with that reported by Azizi et al. (2013) who mention that in the FTIR spectrum of barley husk, the vibration and stress bands of Si-O-Si appear in the regions of 420-500 cm^{-1} and 950-1250 cm^{-1}. The presence of these bands in BHB is due to the high inorganic content of the precursor, which is consistent with the findings of Azizi et al. (2013) and Shen et al. (2014), who report silica content of 80% for barley husk and 60% for rice husk, respectively.

Preprints (www.preprints.org) | NOT PEER-REVIEWED | Posted: 14 December 2017 doi:10.20944/preprints201712.0087.v1

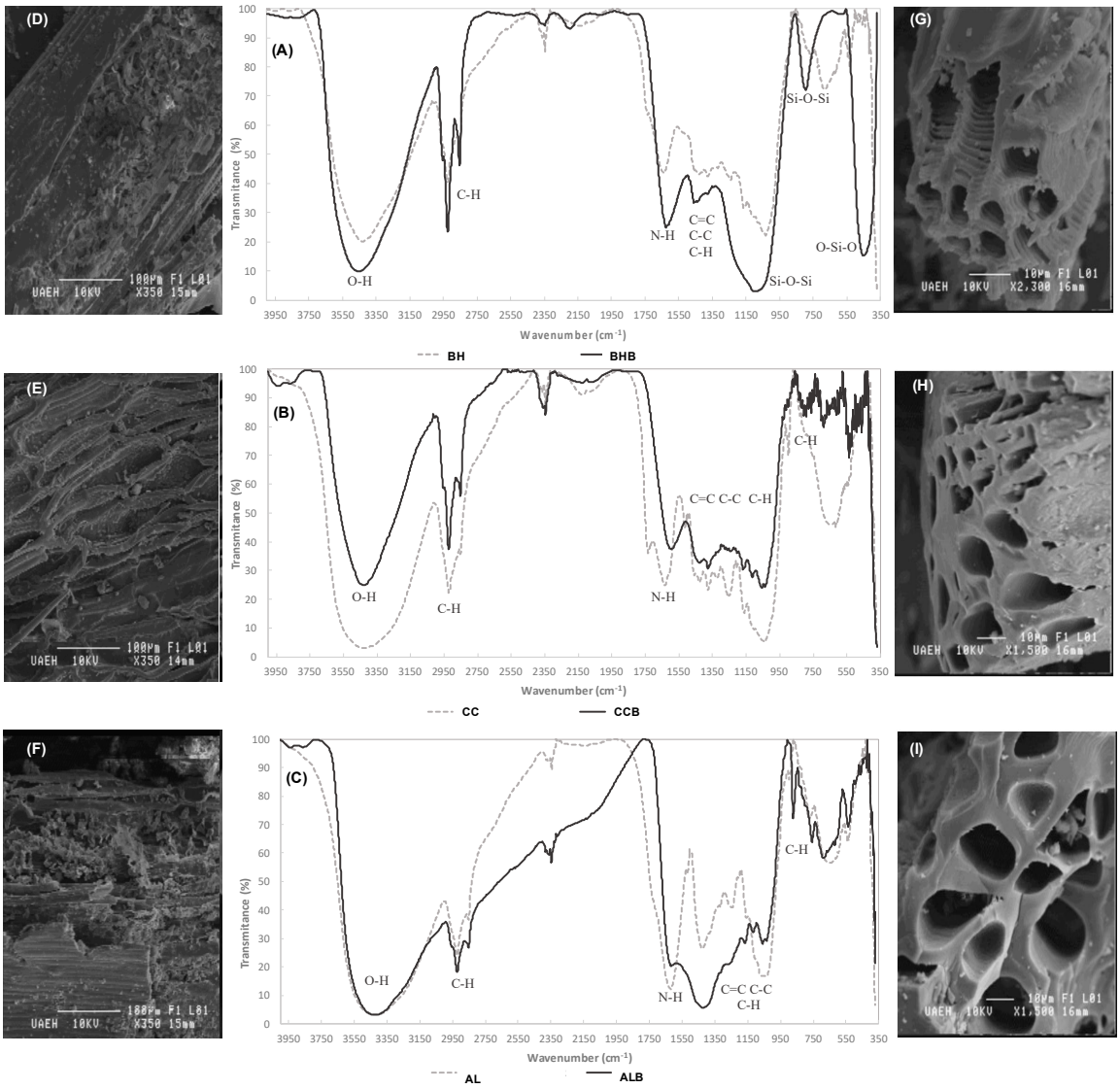

Figure 4. FTIR spectrum of biochars compared with the precursors (A, B, and C). SEM micrographs of precursors (D, E, and F) and biochars (G, H, and I).

3.5. Scanning electron microscopy (SEM)

The morphological changes of the biomass samples, before and after the pyrolysis were observed by scanning electron microscopy.Figure 4 shows the surface morphology of the raw materials (Figure 4D-F) and the biochars (Figure 4G-I). It can be observed that three lignocellulosic residues have fibrous and porous structure, which are suitable characteristics to obtain carbonaceous materials such as activated carbons (Canales-Flores and Prieto-

Preprints (www.preprints.org) | NOT PEER-REVIEWED | Posted: 14 December 2017 doi:10.20944/preprints201712.0087.v1

García, 2016) since biomass can readily decompose and burn. According to the literature, a good precursor of activated carbon must have a porous and fibrous structure, since under this condition, the oxygen can quickly diffuse inside the particle during combustion, and volatile material can be gradually released (Gani and Naruse, 2007). Besides, from the results of the micrographs of the biochars, it is established that the morphology of the biochars obtained depends strongly on the precursor used. Thus, SEM images of the three coals showed the formation of irregular shape and size cavities. It was observed that biochar prepared from BH (Figure 4G) shows eroded particles composed of a large number of channels and some smaller particles adhered to its surface. For CCB, Figure 4H shows irregularly shaped channels with small holes of irregular size and the presence of smaller particles adhered to their surface which occurred as a result of the combustion of the precursor. In Figure 4I, it can be seen that in the ALB channels of regular shapes and variable sizes were obtained.

3.6. Mercury porosimetry

From the results achieved from the micrographs, Figure 5 shows the pore size distribution curves for BHB, CCB, and ALB. The pore sizes were classified according to the pore radius (micropores 1-20 Å, mesopores 20-500 Å, macropores 500-50000 ÅÅ).When we compared the pore size distribution curves for the three biochars, we observed the predominance of macroporous structures in the three carbonaceous materials. As shown in Figure 5, the ALB presented the highest volume of macropores with 0.045 cm^3/g, followed by CCB with 0.037 cm^3/g, and BHB with 0.031 cm^3/g. Therefore, biochars with macroporous structures were obtained under optimal conditions of pyrolysis.

Preprints (www.preprints.org) | NOT PEER-REVIEWED | Posted: 14 December 2017 doi:10.20944/preprints201712.0087.v1

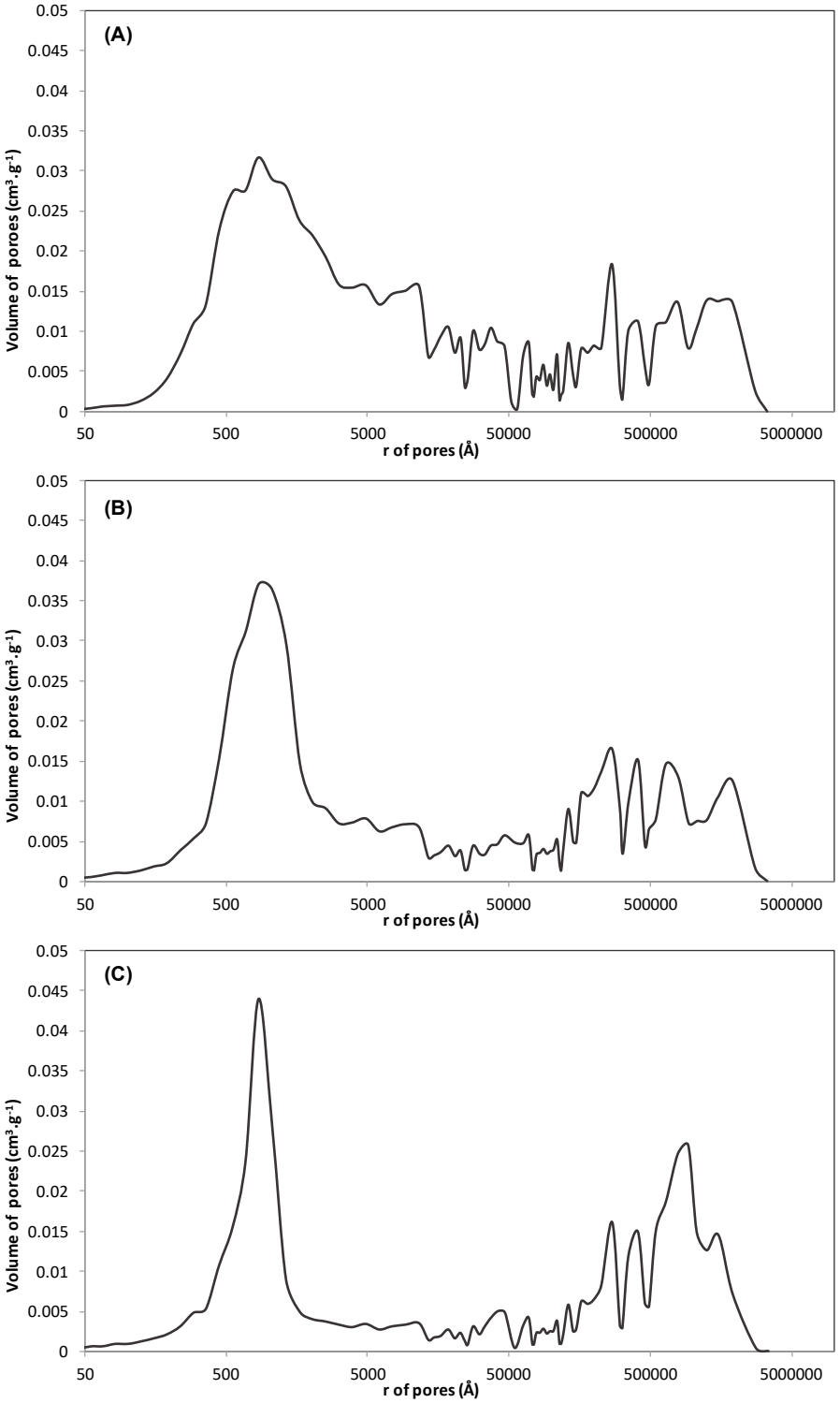

385

386 **Figure 5.** Pore size distribution curve for (A) BHB, (B) CCB, and (C) ALB.

 doi:10.20944/preprints201712.0087.v1

3.7. X-ray diffraction (XRD)

X-ray diffraction patterns of BHB, CCB, and ALB are shown in Figure 6. In the diffraction patterns of the three biochars, the amorphous response is observed from 2θ=10°, resulting from the heat treatment, forming a broad peak which can be attributed to the formation of cross-linked graphitic structures that form the carbon-pore structure. This finding indicates the presence of carbon-pore interfaces in the biochars, which is consistent with those reported by Prías-Barragán et al. (2011).

Peaks for 2θ around 28° and 41° were observed in BHB and CCB, which correspond to the peak (002) and the peak (100) of the graphite structure, respectively. According to Duan et al. (2016), these peaks show graphitization processes during pyrolysis. Thus, it can be established that the graphitization was slight since the peaks are not defined. The authors also explain that the broad peak at (002) could be the result of the incomplete development of microcrystalline structures, and the tiny peak at (100) could be attributed to the disordered graphite layers that were formed during the heat treatment. This second peak was more intense in the CCB (Figure 6B), followed by ALB (Figure 6C) and practically null in BHB (Figure 6A). Therefore, the peaks obtained in the diffractograms are indicative of the formation of graphite layers in the carbonaceous materials, mainly in CCB and ALB.Itcan be deduced from these peaks that the activated carbon is mostlikely amorphous and does not represent a crystalline structure.In contrast, the diffraction pattern of BHB shows peaks at approximately 21º of 2θthan can be associated with the presence of amorphous SiO_2 (Music et al., 2011; Shen et al., 2014). It represents a clear and consistent finding that in BHB are present amorphous silicon oxides.

Preprints (www.preprints.org) | NOT PEER-REVIEWED | Posted: 14 December 2017 doi:10.20944/preprints201712.0087.v1

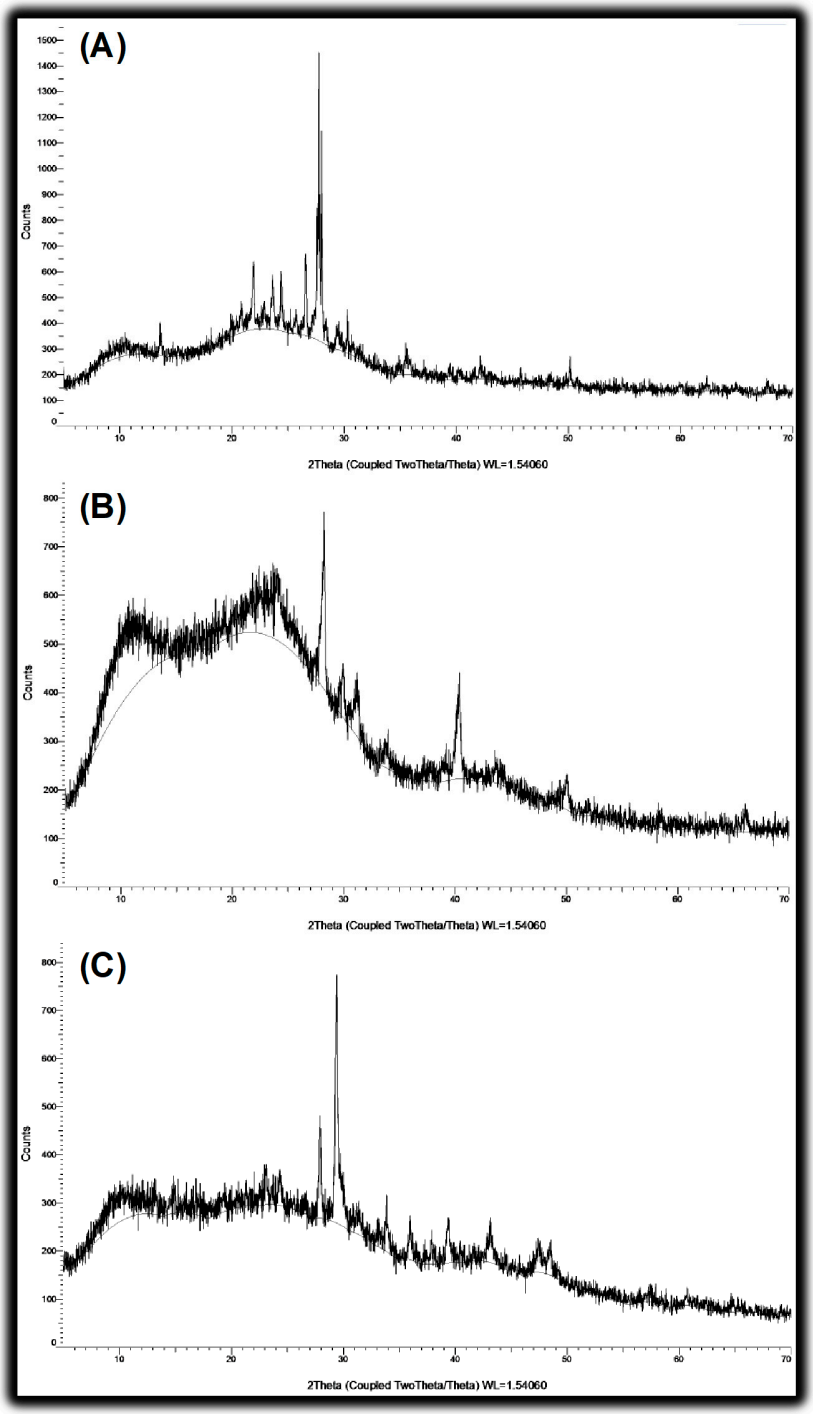

Figure 6. XRD pattern of (A) BHB, (B) CCB, and (C) ALB.

 doi:10.20944/preprints201712.0087.v1

420

421 **3.8. Thermogravimetric analysis (TGA)**

422 As a representative result of the thermogravimetric analysis, Figure 7 and Figure 8 shows
423 profiles of the fraction of the mass decrease of combustibles for precursors and biochars,
424 respectively. The vertical axis represents the fraction of mass decrease of combustibles.
425 From Figure 7, the thermal decomposition of lignocellulosic compounds starts at about 180
426 ºC for all the samples. As shown, the combustibles in the biomass react at the five stages
427 during the thermal decomposition (Nieto-Delgado and Rangel-Méndez, 2013). The first
428 phase at a temperature between 70 °C and 150 °C was attributed to moisture released and to
429 the evaporation of some volatile compounds. The second stage was found from 180 °C to
430 about 230 °C and was attributed to the degradation of hemicellulose. At the third stage, the
431 mass rapidly decreases due to the cellulose volatilization. This stage was observed in the
432 temperature range of 250 ºC to 350 °C for all the samples and was representative of the
433 thermal decomposition of cellulose. Thus, peaks at 299 °C for BH, at 300 °C for CC, and at
434 326 °C for AL were observed. Similar behaviors have been reported in other studies for the
435 same precursors (Bagheri and Abedi, 2009; Bledzki et al., 2010; Nieto-Delgado et al.,
436 2011; Espino et al., 2014). The fourth stage, between 380 °C and 550 °C, was attributed to
437 the lignin decomposition. As shown in Figure 7, the thermogravimetric analysis for BH,
438 CC, and AL demonstrate that cellulose is the major component in all precursors.This result
439 is because the three precursors showed high cellulose content and low lignin content as
440 shown in Table 1.
441 According to Gani and Naruse (2007), the cellulose decomposes in the temperature range
442 of 240-350 °C (Nieto-Delgado and Rangel-Méndez, 2013). In contrast, lignin is the
443 biomass fraction with the higher decomposition temperature (280-500 °C), since part of
444 lignin consists of benzene rings, and is the fraction with higher carbon content (Gani and
445 Naruse, 2007; Nieto-Delgado and Rangel-Méndez, 2013).
446 The fifth stage was attributed to the ash derived from the degradation of complex polymers
447 and inorganic salts present in the precursors, mainly in BH and AL. These results are
448 consistent with those reported by Gani and Naruse (2007) who suggest that the thermal
449 behavior of biomass depends on its components such as the cellulose and lignin content.

Preprints (www.preprints.org) | NOT PEER-REVIEWED | Posted: 14 December 2017 doi:10.20944/preprints201712.0087.v1

In the thermal decomposition profile of the biochars, a very discreet endothermic peak was observed at temperatures below 100 °C, attributed to desorption of physisorbed water (Figure 8). For the biochars sample, the peak corresponding to cellulose and hemicellulose degradation was not observed. It is a difference concerning the thermal decomposition profile of the lignocellulosic residues. Finally, fluctuations occurring between 450 and 550 °C were found in the thermal decomposition profile of biochars which can be attributed toprolonged lignin degradation since this compound has high thermal stability (Figure 8). This peak was more intense in the ALB since its precursor has the highest lignin content as shown in Table 1.

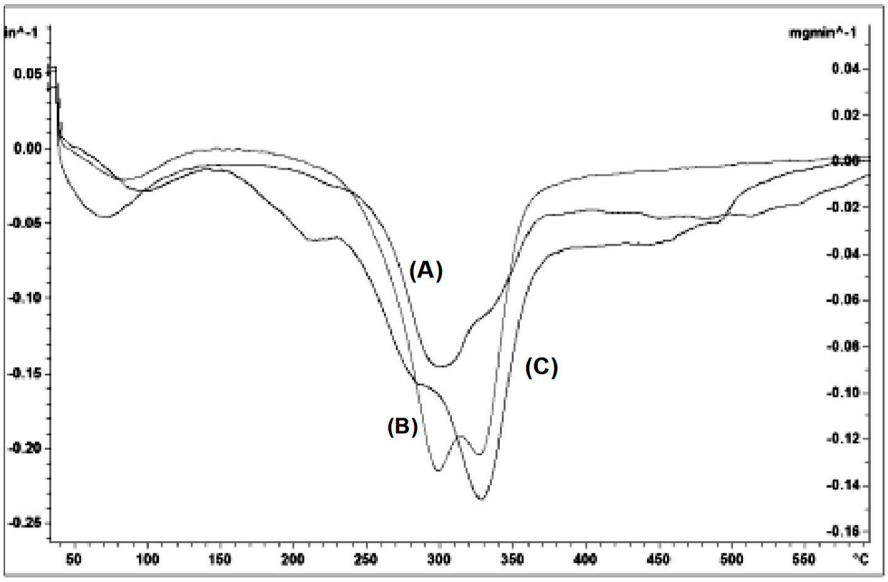

Figure 7. Thermogravimetric analysis of (A) BH, (B) CC, and (C) AL.

Preprints (www.preprints.org) | NOT PEER-REVIEWED | Posted: 14 December 2017 doi:10.20944/preprints201712.0087.v1

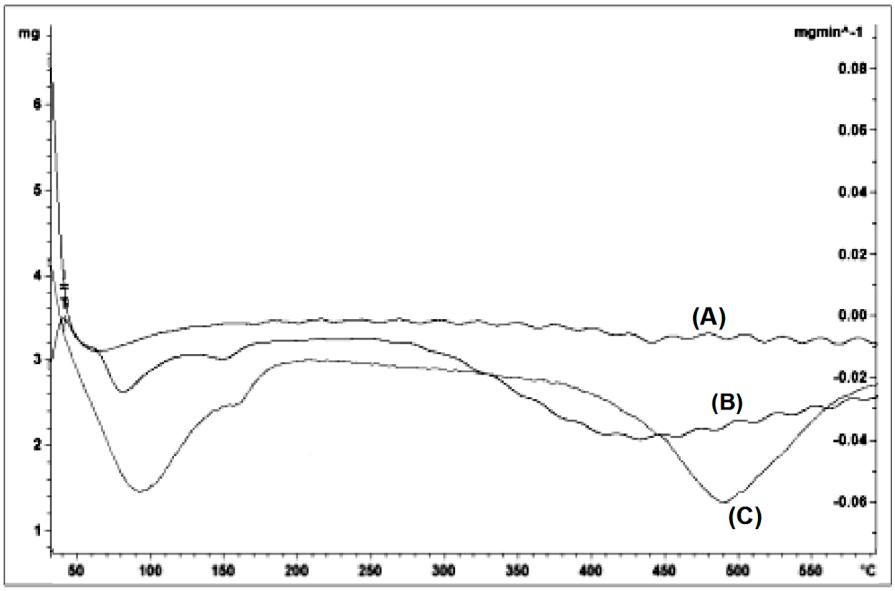

Figure 8. Thermogravimetric analysis of (A) BHB, (B) CCB, and (C) ALB.

3.7. Zeta Potential

The zeta potential is a physical parameter that can be used to quantify the electrical potential of the surface of a solid particle (Li et al., 2003). According to the literature, the electrokinetic behavior of the activated carbons in solution is one of the most important properties in the characterization of these materials. It is also mentioned that these materials are amphoteric due to the presence of several functional groups on their surfaces and to delocalized electrons that confer fundamental properties (Chingombe et al., 2005). Thus, zeta potential measurements determined that the surface charge of the three biochars is anionic, obtaining values of -34.40 mV for BHB, -48.02 mV for CCB, and -29.00 mV for ALB. It can be observed that CCB presented the highest value of anionic surface charge after the pyrolysis process, followed by ALB and ultimately BHB. From these results, it is established that the zeta potential values indicate the presence of anionic surfaces in the biochars obtained, mainly in CCB. Therefore, the biochars achieved in this study can be effective for adsorption processes of molecules or ions with positive surface charge.

Conclusions

Biochars were produced from barley husk, corn cob, and agave leaves. The effectof operating parameters on the biochar yield wasinvestigated. The experiments were based on

Taguchi experimental design (L9). Theanalysis of variance made clear that the leading factor was the activation time with about 50% effect on the biochar yield. The optimumconditions obtained for maximum biochar yields were: carbonization temperature of 400 ºC (level 2), process time of 30 min (level 1), precursor mass of 2 g (level 1), and N_2 flow rate of 150 cc/min (level 2). Biochar yields of 19.75% for CCB, 32.88% for BH, and 31.14% for ALB were obtained at optimum conditions. Biochars with a predominantly macroporous structure, amorphousstructure, numerous oxygen functional groups, anionic surface and moderate ash content were obtained. The results of this investigation show that barley husk, corn cob, and agave leaves are likely precursors for biochar production.

Acknowledgements

This work was supported by the National Council of Science and Technology (CONACyT) [doctorate scholarship number 289880].

References

Ahmad, M., Rajapaksha, A. U., Lim, J.E., Zhang. M., Bolan, N., Mohan, D., Vithanage, M., Lee, S.S., Ok, Y.S. (2014) Biochar as a sorbent for contaminant management in soil and water:A review. *Chemosphere*, **99**:19-33.

ASTM Standard D3172, 1989, 1997. Standard Practice for Proximate Analysis of coal and coke. ASTM International, West Conshohocken, PA.

Ateş, F., Pütün, E., Pütüna, E. (2004) Fast pyrolysis of sesames talk: yields and structural analysis of bio-oil. *J. Anal. Appl. Pyrol.*, **71**:779–790.

Azizi, S.N., Dehnavi, A.R., Joorabdoozha, A. (2013) Synthesis and characterization of LTA nanozeolite using barley husk silica: Mercury removal from standard and real solutions. *Mater. Res. Bulletin*, **48**:1753-1759.

Bagheri, N., Abedi, J. (2009) Preparation of high surface area activated carbon from corn by chemical activation using potassium hydroxide. *Chem. Eng. Res. Des.*,**87**:1059-1064.

511 Bledzki, A.K., Mamum, A.A., Volk, J. (2010) Barley husk and coconut shell reinforced
512 polypropylene composites: The effect of fibre physical, chemical and surface properties.
513 *Compos Sci Technol,* **70**:840-846.
514 Bohli, T., Ouderni, A., Fiol, N., Villaescusa, I. (2015) Evaluation of an activated carbon
515 from olive stones used as an adsorbent from heavy metal removal from aqueous phases.
516 *Comptes Rendus Chimie*, **18**:88-99.
517 Canales-Flores, R. A., Prieto-García, F. (2016) Carbonoceous materials from agricultural
518 waste. A review. *Chem. Biodiversity*, **13**:261-268.
519 Chingombe, P., Saha., B., Wakeman, R.J. (2005) Surface modification and characterization
520 of a coal-based activated carbon. *Carbon*, **43**:3132-3143.
521 Choi, H.S., Choi, Y.S., Park, H.C. (2012) Fast pyrolysis characteristics of lignocellulosic
522 biomass with varying reaction conditions. *Renew Energy*, **42**:131–135.
523 Demirbas, A. (2004) Effect of initial moisture content on the yields of oily products from
524 pyrolysis of biomass. *J. Anal. Appl. Pyrol.,* **71**:803-815.
525 Duan, X., Srinivasakannan, C., Wang, X., Wang, F. Liu, X. (2016) Synthesis of activated
526 carbon fibers from cotton by microwave induced H_3PO_4 activation. *J. Taiwan Inst. Chem.*
527 *Eng.*, **000**:1-8.
528 Espino, E., Cakir, M., Domenek, S., Román-Gutiérrez, A.D., Belgacem, N., Bras, J. (2014)
529 Isolation and characterization of cellulose nanocrystals from industrial by-products of
530 Agave tequilana and barley. *Ind. Crop. Prod.,* **62**:552-559.
531 Gani A., Naruse, I. (2007) Effect of cellulose and lignin content on pyrolysis and
532 combustion characteristics for several types of biomass. *Renew. Energ.,* **32**:649-661.
533 Ioannidou, O., Zabaniotou, A. (2007) Agricultural residues as precursors for activated
534 carbon production-A review. *Renew. Sust. Energ. Rev.*, **11**:1966-2005.
535 Kirby, E.D. (2006) A Parameter Design Study in a Turning Operation Using the Taguchi
536 Method, pp. 1-14.
537 Kundu, A., Gupta, B.S., Hashim, M.A., Redzwan, G. (2014) Taguchi optimization
538 approach for production of activated carbón from phosphoric acid impregnated palm kernel
539 shell by microwaveheating, *J. Clean. Prod.*, xxx: 1-8.
540 Li, Y.-H., Wang, S., Luan, Z., Ding, J., Xu, C., Wu, D. (2003) Adsorption of cadmium(II)
541 from aqueous solution by surface oxidized carbon nanotubes. *Carbon*, **41**: 1057-1062.

 doi:10.20944/preprints201712.0087.v1

542 Loloide, Z., Mozaffarian, M., Solieman, M., Asassian, N. (2016) Carbonization and CO2
543 activation of scrap tires:Optimization of specific surface area by the Taguchi method,
544 *Korean J. Chem. Eng.*, xxxx:1-10.
545 Musić, S., Filipović-Vinceković, N., Sekovanić, L. (2011) Precipitation of amorphous SiO_2
546 particles and their properties. *Brazil. J. Chem. Eng.*, **28**: 89-94.
547 Nieto-Delgado, C., Rangel-Méndez, J.R. (2013). Preparation of Carbon Materials from
548 Lignocellulosic Biomass. In: Rufford TE (ed) Green Carbon Materials. Advanced and
549 Aplications, Taylor & Francis Group, US, pp. 51.
550 Nieto-Delgado, C., Terrones, M., Rangel-Mendez, J. R. (2011) Development of highly
551 microporous activated carbon from the alcoholic beverage industry organic by-products.
552 *Biomass Bioenerg.,***35**:103-112.
553 Onay, O., Beis, S.H., Koçkar, O.M. (2001) Fast pyrolysis of rape seed in a well-swept
554 fixed- bed reactor. *J. Anal. Appl. Pyrol*, **58**:995–1007.
555 Pereira, R.G., Martins, C., Mendes, N., Farias, L., Ferreira, R.C., Oliveira, A., Oliveira, M.,
556 da Costa,R. (2014) Preparation of activated carbons from cocoa shells and siriguela seeds
557 using H_3PO_4 and $ZnCl_2$ as activating agents for BSA and α-lactalbumin adsorption. *Fuel*
558 *Process. Technol.,***126**:476-486.
559 Pütün, A.E., Apaydin, E., Pütün, E. (2002) Bio-oil production from pyrolysis and steam
560 pyrolysis of soy bean-cake: product yields and composition. *Energy*, **27**:703–713.
561 Prías-Barragán, J. J., Rojas-González, C. A., Echeverry-Montoya, N. A., Fhontal, G.,
562 Ariza-Calderón, H. (2011) Identificación de las variables óptimas para la obtención de
563 carbón activado a partir del precursor Guadua Angustifolia Kunth. *Rev. Acad. Colomb.*
564 *Cienc.*, **35**:157-166.
565 Sensöz S., Angin D. (2008) Pyrolysis of safflower (Charthamus tinctorius L.) seed press
566 cake: part1. The effects of pyrolysis parameters on the product yields. *Bioresour. Technol.*,
567 **99**:5492–5497.
568 Shen, Y., Zhao, P., Shao, Q. (2014) Porous silica and carbon derived materials from rice
569 husk pyrolysis char. *Micropor. Mesopor. Mat.*, **188**:46-76.
570 Stefanidis, S.D., Kalogiannis, K.G., Iliopoulou, E.F., Michailof, C.M., Pilavachi, P.A.,
571 Lappas, AA. A study of lignocellulosic biomass pyrolysis via the pyrolysis of cellulose,
572 hemicellulose and lignin. *J. Annal. Appl. Pyrol.*, **105**:143-150.

573 Shackley, S., Carter, S., Knowles, T., Middelink, E., Haefele, S., Sohi, S., Cross, A.,
574 Haszeldine, S. (2012) Sustainable gasification-biochar systems? A case-study of rice-husk
575 gasification in Cambodia, Part 1: Context, chemical properties, environmental and health
576 and safety issues. *Energ. Policy,***42**: 49–58.
577 Syed-Hassan, S.S.A., Md Saini, M.S. (2016) Optimization of the preparation of activated
578 carbon from palm kernel Shell for methane adsorption using Taguchi orthogonal array
579 design. *Korean J. Chem. Eng.*, xxxx:1-11.
580 TAPPI T203 (1999) Alpha-, beta- and gamma-cellulose in pulp. TAPPI Press, Norcross,
581 Georgia.
582 TAPPI T204 (1997) Solvent extractives of wood and pulp. TAPPI Press, Norcross,
583 Georgia.
584 TAPPI T222 (1998) Acid-insoluble lignin in wood and pulp. TAPPI Press, Norcross,
585 Georgia.
586 Tripathi, M., Sahu, J.N., Ganesan, P. (2016) Effect of process parameters on production of
587 biochar from biomass waste through pyrolysis: A review. *Renew. Sust. Energ. Rev.*,
588 **55**:467-481.
589 Wise L.E., Marphy M., d'Adieco A. (1946) A chlorite holocellulose, its fractionation and
590 bearing on summative wood analysis and studies on the hemicelluloses. *Pap. Trade.*
591 *J.***122**:35-43.
592 Xiong, S., Zhuo, J., Zhang, B., Yao, Q. (2013) Effect of moisture content on the
593 characterization of products from the pyrolysis of sewage sludge. *J. Anal. Appl.*
594 *Pyrol.***104**:632-639.
595 Zhang H., Xiao R., Huang H., Xiao G. (2009) Comparison of non-catalytic and catalytic
596 fast pyrolysis of corn cob in a fluidized bed reactor. *Bioresour. Technol.*, **100**:1428–1434.